Journal of Sol-Gel Science and Technology 36, 257–264, 2005

DOI: 10.1007/s10971-005-4510-3

Preparation of Titania/PDMS Hybrid Films and the Conversion to Porous Materials

MASATO NAKADE
Research and Development Division, KOSÉ Corporation, Azusawa 1-18-4, Itabashi-ku, Tokyo 174-0051, Japan

KOSUKE ICHIHASHI
School of Science and Engineering, Waseda University, Nishi-waseda 1-6-1, Shinjuku-ku, Tokyo 169-8050, Japan

MAKOTO OGAWA*
School of Science and Engineering, Waseda University; Department of Earth Sciences, Waseda University,
Nishi-waseda 1-6-1, Shinjuku-ku, Tokyo, 169-8050, Japan
makoto@waseda.jp

Received April 25, 2005; Accepted August 22, 2005

Abstract. Transparent films of titania/poly(dimethylsiloxane) (PDMS) hybrids were prepared by the solvent evaporation from the precursor solution prepared by the co-hydrolysis and co-condensation of titanium tetraisopropoxide and a methoxy-functionalized PDMS. The hybrid films were flexible and had high homogeneity of the composition. The organic groups of PDMS were decomposed at 400°C in air to form porous films. Though the heated films were rather brittle compared to the as-synthesized films, they were still transparent and homogeneous. The BET surface areas of the films after the heat treatment at 400°C were over 300 m^2/g, while the as-synthesized hybrid films were non porous. According to the BDDT classification, the nitrogen adsorption/desorption isotherms of the calcined films were Type I, showing that the films were microporous. The titania domains were still amorphous after the heat treatment at 400°C and transformed to anatase after the heat treatment at 1,000°C.

Keywords: titania, silicone, hybrid, thermal decomposition, microporous

Introduction

Titania-containing composite materials have attracted considerable attention because of their useful properties such as photocatalytic ones, optical properties utilizing the high refractive index, transparency in the visible light wavelength region, and a characteristic absorption in the UV wavelength region. Among reported titania-containing materials, titania-containing silicas and silicates of both porous and nonporous ones are of practical interests due to the versatility of the nanostructures and the chemical and thermal stabilities. Accordingly, titania-containing silicas and silicates with a wide variety of microstructures and compositions have been synthesized by various chemical means and their properties have been well documented [1–14]. Their microstructures are the topic of interest because they significantly affect the properties of the materials.

We have already reported the synthesis of the spherical titania/poly(dimethylsiloxane) (PDMS) hybrid particles from sols containing titania and oligomeric silicone and the products have been used for a cosmetic

---

*To whom correspondence should be addressed.

application [15]. The hybrid particles have an islet-like nanostructure, which consist of titania and PDMS domains of nanometer size, namely, nanometer size titania particles are supported by the silicone. More recently, we have reported the thermal decomposition of the titania/PDMS hybrid particles and successfully prepared microporous titania/silica particles, which retained the original spherical morphology [16]. The successful transformation of the nanostructures with retaining particle morphology encourages us to study the preparation of titania/PDMS hybrids with various controlled morphology. Here, we report the preparation of titania/PDMS hybrid films and the transformation to microporous films by the thermal decomposition of the silicone. Film is an ideal morphology for optical characterization and certain applications. Oxide containing silicone films have been synthesized for the applications to the surface modification or functionalization of glasses [17] and plastics [18], separation membrane [19–21] and so on [22]. The present syntheses are applicable approaches for such purposes due to the ease of operation and versatility of the composition. Recently, Shindou et al. have reported the coating of PDMS-based hybrid, which was synthesized from titanium tetraisopropoxide (TTP) and PDMS, on polyimide sheet for electrophotographic printers [23, 24]. The surface properties of the coatings have been investigated by means of contact angle measurements and AFM. In the present paper, our attention is focused on the preparation and characterization of "self-standing" titania/PDMS hybrid films with the thickness of several tens of μm from TTP and methoxy functionalized PDMS, and the conversion to porous films by the heat treatment in air.

Experimental

Materials

Titanium tetraisopropoxide (TTP) (Wako 1st grade 95 wt%+) was purchased from Wako Pure Chemical Ind., Ltd., 2-Propanol (analytical grade) and hydrochloric acid aqueous solution (35 wt%) were purchased from Kanto Chemical Co., Inc. (Tokyo, Japan). Methoxy-functionalized PDMS with a number-average molecular weight of 1080 (Scheme 1) was supplied by Shin-Etsu Chemical Co., Ltd. (Tokyo, Japan). These chemicals were used without further purification.

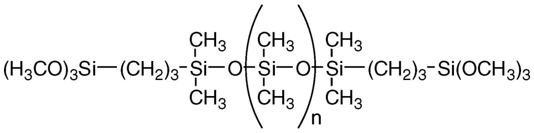

$$(H_3CO)_3Si-(CH_2)_3-Si(CH_3)_2-O-\left(Si(CH_3)_2-O\right)_n-Si(CH_3)_2-(CH_2)_3-Si(OCH_3)_3$$

Scheme 1. Chemical structure of the methoxy-functionalized polydimethylsiloxane.

Sample Preparation

According to the method reported by Wang et al. [25], transparent titania sol was synthesized by slowly adding distilled water and hydrochloric acid aqueous solution diluted with 2-propanol to TTP at room temperature. The molar ratio of TTP, water, and hydrochloric acid was 1:1:0.06, and the amount of 2-propanol was 400 ml for 1 mol of TTP. The sols containing titanium dioxide and oligomeric PDMS were prepared by mixing the titania sols with 21.0 g of methoxy-functionalized PDMS diluted with 20 ml of 2-propanol, where the molar ratios of TTP and methoxy-functionalized PDMS were 10:1, 5:1 and 2.5:1, abbreviated as TS (10), TS (5), and TS (2.5) respectively. 2 ml of the sol was deposited on poly(ethylene) film which was stretched on the underside of glass petri dish (76 cm^2) and dried in air at ambient temperature for 1 day to remove the solvent and to complete the condensation of the alkoxides. The dried films were peeled off from the substrates, yielding transparent and flexible films. Then the films were heated at 400°C in air (with the heating rate of 10°C/min) for 1 h in order to decompose the organic groups. For TS (10), the duration was varied from 1 to 24 h.

Characterization

The images of the films were obtained by scanning electron microscopy (SEM) (JEOL, JSM-6301F) equipped with an energy-dispersive X-ray spectroscopy (EDS) system. The films were coated with platinum by an ion sputter (JEOL JFC-1600). For the observation of the cross section, the as-synthesized film was embedded in an epoxy resin matrix (Quetol 812; Nissin EM), and cut by a razor to expose the cross section of the film. This resin block including the film was also coated with platinum before the SEM observation. The chemical compositions of the films were determined by an electron probe micro analyzer (EPMA) (JXA-733, JEOL). Fourier transform infrared (FT-IR) spectra of the films were measured with a Shimadzu

FT/IR-8200PC in the range of 4000–400 cm^{-1}. X-Ray diffraction (XRD) patterns were obtained with Rigaku RADIIB (Cu Kα) operated at 40 kV and 20 mA in the $2\theta = 5$–60° range. Differential thermal analysis (DTA) and thermogravimetric analysis (TG) were carried out from room temperature to 1,000°C in air at a heating rate of 10°C/min using TA-200 (Rigaku). N_2 adsorption/desorption isotherms of the films at 77 K were obtained by BELSORP 28 (Bel Japan Inc.). Before the measurements, samples were evacuated in vacuum for 3 h at 120°C. The pore size was estimated by BJH method [26]. CHN elemental analysis was performed by Perkin Elmer 2400II. Ultraviolet and visible (UV-Vis.) absorption spectra of the films were recorded on a UV-Vis. spectrometer (UV-3100PC, Shimadzu) in the range of 200–800 nm.

Results and Discussion

Synthesis of Titania/PDMS Hybrid Films

As-synthesized films were transparent and flexible with the thickness of ca. 10 μm. As a typical example, a photograph and a SEM image of the as-synthesized film TS (10) are shown in Figs. 1 and 2(a), respectively. The titania and PDMS phases were mixed very homogeneously at a nanometer scale, so that no phase separation between the titania phase and the PDMS phase was observed by the SEM observation even at a very high magnification (∼100,000×). In our separate study on the preparation and characterization of titania/PDMS hybrid particles, it was also impossible to observe the titania/PDMS interface by the SEM observation [15]. By means of EPMA, it was confirmed that the Ti/Si ratios of the as-synthesized films corresponded to that of the starting solutions (Ti/Si = 0.21–0.83) and were constant throughout the in-plane of the films (data were not shown). The Ti/Si ratios of the hybrid films previously reported by Shindou et al. [24] were in the range of about 0.025 to 0.063, which were estimated from an average molecular weight of PDMS they used. Compared with the reported materials, the present hybrids contained higher amount of Ti. The Ti content is an advantage of the present hybrids films for a certain kind applications such as photocatalytic and UV shielding ones.

In order to confirm the homogeneity in the direction of the thickness, a line analysis was performed in a cross section of the TS (10) film with a SEM/EDS system. The intensity profiles of the characteristic X-rays of Ti and Si superimposed in the SEM image demonstrated that the concentrations of Ti and Si were constant within the film (Fig. 3). Based on the above results, we concluded that titania and PDMS are hybridized at a nanometer scale at least within the range of the spatial resolutions of the present SEM and EPMA observations. On the other hand, Shindou et al. found that the hybrids on polyimide sheets after the heat treatment at 150°C had the continuous-phase structure (lamellar structure) or "sea-island" structure in a micrometer scale due to the phase separation [24]. The difference in the microstructure was ascribed to the difference in the starting materials and the synthetic processes.

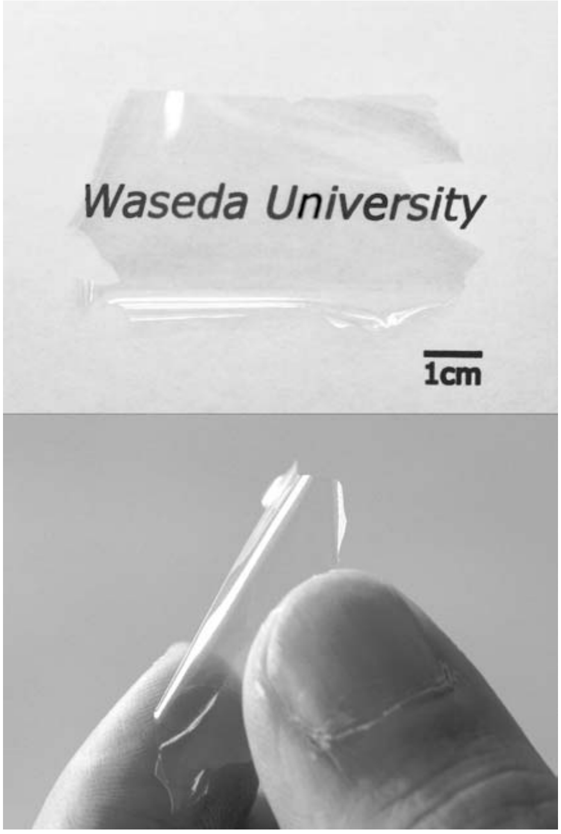

Figure 1. Photographs of the as-synthesized film (TS (10)).

No diffraction peak due to any crystalline phases was observed in the XRD patterns of the as-synthesized films. In the IR spectrum of TS (10) (Fig. 4(a)), the absorption bands due to silicone appear at 1263 cm^{-1} (CH_3 bending vibrations), 1099 and 1026 cm^{-1} (Si-O stretching vibrations) [27]. At the low wavenumber region, a broad absorption band due to an envelope of

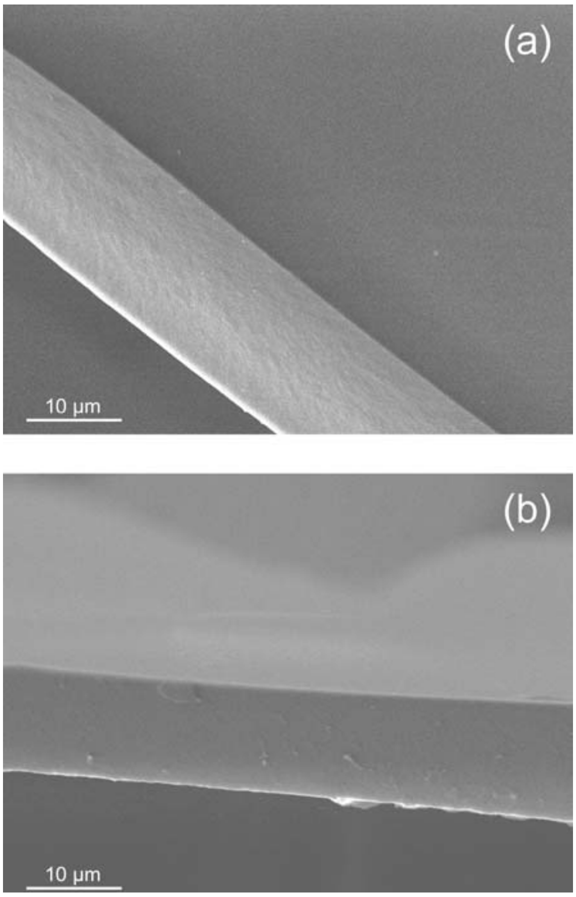

Figure 2. SEM images of TS (10) before and after the heat treatment; (a) as-synthesized film, (b) 400°C, 1 h.

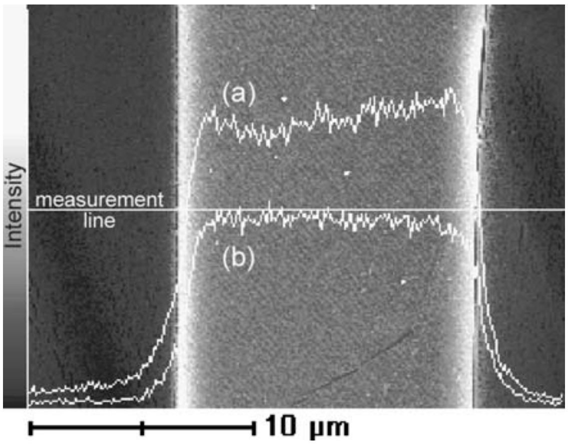

Figure 3. SEM image of a cross section of the as-synthesized film TS (10) with the result of line analysis by an EDS system. The curves superimposed on the SEM image represent the intensity profiles of the characteristic X-rays of (a) Si and (b) Ti.

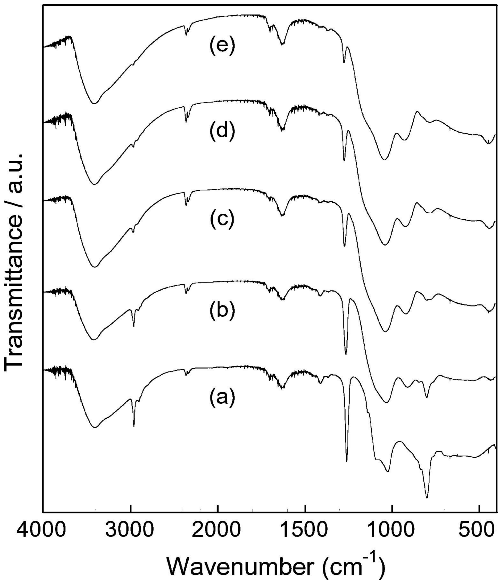

Figure 4. IR spectra of TS (10) before and after the heat treatment at 400°C; (a) As-synthesized, (b) 1 h, (c) 5 h, (d) 7 h, (e) 24 h.

Ti-O-Ti bond was observed. As a whole, the profile of the spectrum was an overlapping of the separate absorptions due to titanium dioxide and PDMS. The profiles of IR spectra of TS (5) and TS (2.5) were essentially similar to that of TS (10) except the intensities of absorption band of silicone, which corresponded to the ratio of silicone to titania. However, the absorption bands (around 920–960 cm^{-1}) ascribable to Si-O-Ti bond, which have been observed for the composite materials of titania and silicone [28] or silica [29], was not observed in the as-synthesized sample. The absorption band due to Si-O-Ti in the present system might be masked by the bands due to Si-CH$_3$ and Ti-O-Ti bonds because the amounts of Si-O-Ti bonds at the interface of titania and silicone domains were relatively small.

Figure 5 shows the UV-Vis. absorption spectra of the films. The absorption edge derived from the spectra suggested that the Ti atoms form titania domains rather than to be isolated ions in the present system. The absorption edges determined from the spectra were observed at lower wavelength regions relative to that of anatase (385 nm). The absorption bands shifted to shorter wavelength regions from 341 to 334 nm as the titania contents decreased from Ti/Si = 0.83 (TS (10)) to 0.21 (TS (2.5)). These observations as well as previously mentioned microscopic observations indicated that the sizes of the titania phases are small so that a quantum size effect caused the spectral blue shift.

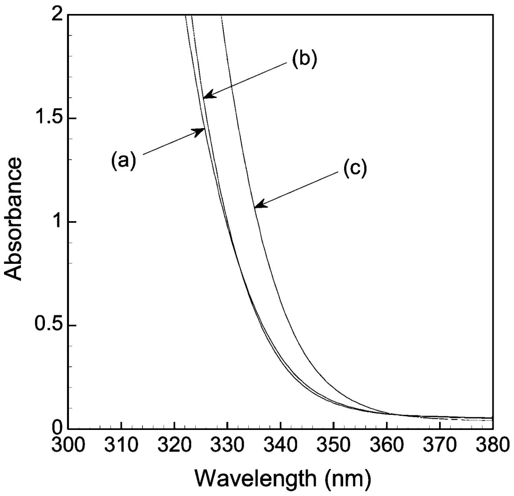

Figure 5. UV-Vis. spectra of the as-synthesized films; (a) TS (2.5), (b) TS (5), (c) TS (10).

Thermal Decomposition of the Titania/PDMS Hybrid Films

Figure 6 shows the TG and DTA curves of the as-synthesized film TS (10). The curve profiles were identical to that of the titania/PDMS hybrid particles reported previously [16]. Weight losses due to the desorption of remaining solvents and the thermal decomposition of the silicone were observed below 700°C in the TG curve and a broad exothermic peak started from 200°C and centered at 400°C, which was mainly attributed to the combustion of methyl and methylene groups of the silicone, was observed in the DTA curve. Another exothermic peak was seen at around 640°C and no other specific reaction was observed at higher temperature range in the DTA curve. XRD measurements were performed for the sample after the heat treatment at 500, 700 and 1000°C. There was no recognizable diffraction peak in XRD patterns for 500 and 700°C. On the other hand, diffraction peaks due to anatase were seen for the sample after the heat treatment at 1000°C. These results suggested that titania domains transformed to anatase above 700°C. The origin of the exothermic peak at around 640°C in the DTA curve was not clear at this stage. The TG-DTA results suggest that heat treatments at different temperatures and periods may result in products with different composition and porosity. In the present study, the thermal treatment was conducted at 400°C, and the duration was varied to control the composition and microstructure for TS (10).

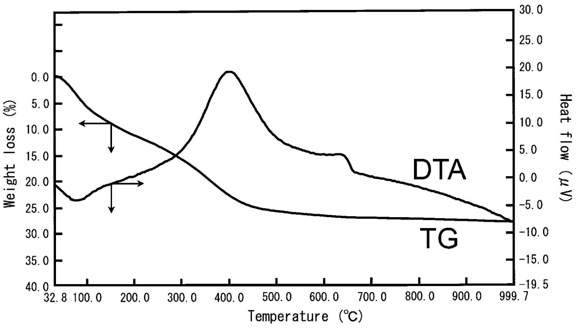

Figure 6. TG-DTA curves of the as-synthesized film TS (10).

The films after the heat treatment at 400°C for 1 to 24 h were transparent. The shapes were kept after the heat treatment. The films lost their flexibility and became more brittle as the heat treatment time became longer. Figure 2b shows a SEM image of the TS (10) after the heat treatment at 400°C for 1 h. There was no recognizable phase separation same as those observed for the as-synthesized films. Comparing with the as-synthesized film (Fig. 2a), the cross section area of the calcined film was smoother than the as-synthesized sample, in other words, the calcined film had glassy looking. Meanwhile, no obvious peak was found in the XRD patterns of the calcined films, indicating that these films were also X-ray amorphous. Very similar results were obtained for the films heated for longer period.

The nitrogen adsorption-desorption isotherms of the films before and after the heat treatment were recorded to evaluate the porosity. The surface areas were calculated using the BET equation and the results are presented in Table 1. The isotherms of the as-synthesized films were Type III according to the BDDT classification and their BET surface areas were virtually 0 m^2/g, indicating the as-synthesized films were nonporous. On the other hand, the BET surface areas of the films markedly increased after the heat treatment at 400°C for 1 h. The nitrogen adsorption isotherms for the films after the heat treatment were Type I, showing the micro pore was generated by the heat treatment. It was attempted to determine the pore sizes by the BJH method, however there was no peak in the pore size distribution. At present, we assume that the pore with the size of less than 2 nm formed in the heated films.

The BET surface areas of the films after the heat treatment for 1 h were 276, 325 and 323 m^2/g for TS (10), TS (5) and TS (2.5), respectively as depicted in Table 1. TS (2.5) and TS (5), which had higher ratio of silicone phase relative to TS (10), had higher BET surface areas than TS (10) after the heat treatment. However, when the BET surface areas were converted to the area per the weight of silicone in the films, the areas were 517, 467 and 394 m^2/g-silicone for TS (10), TS (5) and TS (2.5), respectively. These micropores were thought to be generated by the decomposition of the organic groups of the silicone phase.

The BET surface areas for TS (10) when the duration time varied are shown in Table 2. For the sample after the heat treatment for 7 h, the BET surface area was over 300 m^2/g. The BET surface area decreased to 226 m^2/g after the heat treatment for 24 h. The carbon contents of the films determined by the elemental analysis are also summarized in Table 2. The carbon content decreased gradually with the prolonged heat treatment, indicating that the organic groups decomposed gradually. Taking the nitrogen adsorption-desorption isotherms into consideration, it is postulated that the decomposition of the organic groups of the silicone phase occurs along with the generation of the micropores. Further heat treatment led the collapse of the generated micropores due to the densification.

The variation of IR spectra of the films with the heat treatment at 400°C supported the above-mentioned discussion on the decomposition of the organic groups of the silicone phase. Figure 4 shows the IR spectra of TS (10) before and after the heat treatment at 400°C. The bands due to Si-CH$_3$, 1401 cm^{-1} (asymmetric bending vibration), 1261 cm^{-1} (symmetric bending vibration) and 801 cm^{-1} (Si-CH$_3$ stretching and CH$_3$ rocking vibration mode), decreased sequentially by the heat treatment at 400°C for different durations. Furthermore, the contribution of the absorption bands at 2965 and 2906 cm^{-1} due to CH$_3$ and CH$_2$ asymmetric stretching vibrations also decreased by the heat treatment.

Table 1. BET specific surface area and carbon content of the titania/PDMS hybrid films treated at 400°C for 1 h.

	BET specific surface area (m^2/g)	Carbon content (%)
TS (10)	276	8.5
TS (5)	325	10.9
TS (2.5)	323	10.8

Table 2. BET specific surface area and carbon content of the TS (10) treated at 400°C

Treatment time	BET specific surface area (m^2/g)	Carbon content (%)
1 h	276	8.5
5 h	265	4.8
7 h	302	4.4
24 h	226	2.8

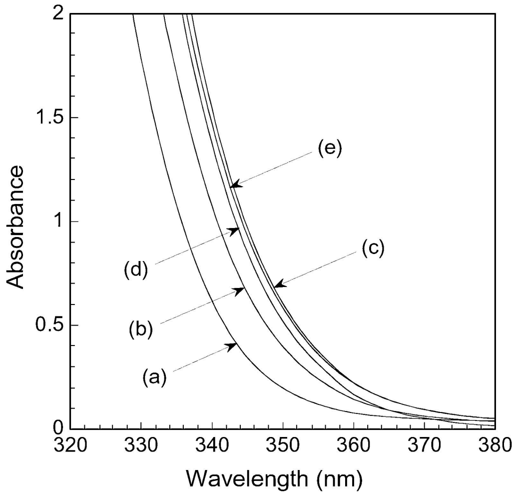

Figure 7. UV-Vis. spectra of TS (10) before and after the heat treatment at 400°C; (a) as-synthesized film, (b) 1 h, (c) 5 h, (d) 7 h, (e) 24 h

The bands related to the framework of the silicone phase changed by the heat treatment. The bands around 1026 and 1099 cm^{-1} due to Si-O asymmetric stretching vibration in the spectrum of the as-synthesized film appeared to be a single broad absorption band at 1030–1040 cm^{-1} with a shoulder at a higher wave number region after the heat treatment. A weak band appeared at around 440 cm^{-1} after the heat treatment and the band was attributed to the rocking motions of the oxygen atoms perpendicular to the Si-O-Si plane [4, 30]. These changes in the IR spectrum of the film, which are similar to that of the particulate form [16], demonstrate that the silicone phase transformed to silica by the decomposition of the organic groups of the silicone. Additionally, a new band appeared at 910–930 cm^{-1} after the heat treatment. For silica-titania composites, absorption bands around this wavenumber region have been ascribed to Si-O$^-$ superimposed on Si-O-Ti [29]. We speculate that the amount of Si-O-Ti bond at the interface of the titania domains and the silicone phase increased, and the absorption band which was masked for the spectrum of the as-synthesized condition became recognizable by the heat treatment at 400°C.

Figure 7 shows the UV-Vis. spectra of TS (10) before and after the heat treatment. The absorption edges were 341 nm for the as-synthesized film and 343, 344, 344 and 344 nm for the films after the heat treatment for 1, 5, 7 and 24 h, respectively. Such small spectral shift is difficult to attribute to the change in the particle size. We thought that the spectral shift reflected the change in the restructure at the titania-silicone interface, however, we do not have any direct evidence at present.

Thus, transparent microporous films containing titania were obtained by the thermal decomposition of the organic groups of the titania/PDMS hybrid films. It is worth noting as a merit of the present synthesis that the amount of titania vary depending on the amount of TTP in the precursor solutions and that the amount of titania was about half of the film by weight for TS (10). Silicones with other organic functionalities are available and it may be possible to affect the pore size corresponding to the size of the substituents [31]. Such kind of films may find applications as UV absorber, photocatalyst, adsorbent and gas separation membrane. Further studies on the synthesis of hybrids with different silicones and composition and the properties of them are further worth conducting.

Conclusions

Titania/poly(dimethylsiloxane) (PDMS) hybrids were prepared as transparent, homogeneous, and flexible films by the solvent evaporation from the precursor solution prepared by the co-hydrolysis and co-condensation of titanium tetraisopropoxide and methoxy-functionalized PDMS. The films were converted into transparent microporous films with a BET surface area of approximately 300 m^2/g by the heat treatment at 400°C in air. The heat treatment caused the thermal decomposition of organic groups of the silicone, resulted in the generation of micropores and the transformation of the silicone to silica, while the transparency of the films was retained.

Acknowledgments

This work was supported by a Grant-in-Aid for Scientific Research on Priority Areas (417) from the Ministry of Education, Culture, Sports, Science and Technology (MEXT) of the Japanese Government and Tokuyama Science Foundation.

References

1. C.J. Brinker and G.W. Sherer, *Sol-Gel Science: The Physics and Chemistry of Sol-Gel Processing* (Academic Press Inc., San Diego, 1990).
2. R.J. Davis and Z. Liu, Chem. Mater. **9**, 2311 (1997).
3. Z. Liu and R.J. Davis, J. Phys. Chem. **98**, 1253 (1994).
4. C.M. Whang and S.S. Lim, Bull. Korean Chem. Soc. **21**, 1181 (2000).
5. Z. Ding, G.Q. Lu, and P.F. Greenfield, J. Phys. Chem. B **104**, 4815 (2000).
6. H.Y. Zhu, J.A. Orthman, J.-Y. Li, J.-C. Zhao, G.J. Churchman, and E.F. Vansant, Chem. Mater. **14**, 5037 (2002).
7. M. Ogawa, K. Ikeue, and M. Anpo, Chem. Mater. **13**, 2900 (2001).
8. Y. Abe, N. Sugimoto, Y. Nagano, and T. Misono, J. Non-Cryst. Solids **104**, 164 (1988).
9. J.B. Miller, S.T. Johnson, and E.I. Ko, J. Catalysis **150**, 311 (1994).
10. E. Lotero, D. Vu, C. Ngyuen, J. Wagner, and G. Larsen, Chem. Mater. **10**, 3756 (1998).
11. W. Que, Z. Sun, Y.L. Lam, Y.C. Chan, and C.H. Kam, J. Phys. D: Appl. Phys. **34**, 471 (2001).
12. J. Sterte, Clays and Clay Miner. **34**, 658 (1986).
13. S. Yamanaka, T. Nishiyama, M. Hattori, and Y. Suzuki, Mater. Chem. Phys. **17**, 87 (1987).
14. Z. Ding, H.Y. Zhu, G.Q. Lu, and P.F. Greenfield, J. Colloid. and Interface Sci. **209**, 193 (1999).
15. M. Nakade, K. Kameyama, and M. Ogawa, J. Mater. Sci. **39**, 4131 (2004).
16. M. Nakade, K. Ichihashi, and M. Ogawa, J. Porous Mater. **12**, 79 (2005).
17. H. Schmidt, J. Non-Cryst. Solids **178**, 302 (1994).
18. M.S. Lee and N.J. Jo, J. Sol-Gel Sci. Technol. **24**, 175 (2002).
19. M.A. LaPack, J.C. Tou, V.L. McGuffin, and C.G. Enke, J. Membr. Sci. **86**, 263 (1994).
20. N.M. Jose, L.A.S.A. Prado, and I.V.P. Yoshida, J. Polym. Sci. Part B: Polymer Physics **42**, 4281 (2004).
21. S. Dirè, E. Pagani, R. Ceccato, and G. Carturan, J. Mater. Chem. **7**, 919 (1997).
22. N. Yamada, I. Yoshinaga, and S. Katayama, J. Sol-Gel Sci. Technol. **17**, 123 (2000).
23. T. Shindou, S. Katayama, N. Yamada, and K. Kamiya, J. Sol-Gel Sci. Technol. **27**, 15 (2003).
24. T. Shindou, S. Katayama, N. Yamada, and K. Kamiya, J. Sol-Gel Sci. Technol. **30**, 229 (2004).
25. B. Wang and G.L. Wilkes, J. Polym. Sci.: Part A: Polym. Chem. **29**,, 905 (1991).
26. E.P. Barrett, L.G. Joyner, and P.P. Halenda, J. Am. Chem. Soc. **73**, 373 (1951).
27. (a) A. Lee Smith, Spectrochim. Acta **16**, 87 (1960), (b) A. Lee Smith, Spectrochim. Acta **19**, 849 (1963), (c) A. Lee Smith,

Analysis of Silicones (Krieger Publishing Company, Florida, 1984)

28. B. Wang, A.B. Brennan, H. Huang, and G.L. Wilkes, J. Macromol. Sci.-Chem. **A27**, 1477 (1990).
29. J.B. Miller, L.J. Mathers, and E.I. Ko, J. Mater. Chem. **5**, 1759 (1995).
30. S. Dirè, R. Campostrini, and R. Ceccato, Chem. Mater. **10**, 268 (1998).
31. G. Larsen, M. Buechler-Skoda, C. Nguyen, D. Vu, and E. Lotero, J. Non-Cryst. Solids **279**, 161 (2001).